Molecular Crystals and Liquid Crystals
Publication details, including instructions for authors and subscription information:
http://www.informaworld.com/smpp/title~content=t713644168

Conducting Polymeric Nanocomposites: Preparation and Evaluation of Structural and Electromagnetic Properties

J. Jiang[a]; L. H. Ai[a]
[a] Chemical Synthesis and Pollution Control Key Laboratory of Sichuan Province, College of Chemistry and Chemical Engineering, China West Normal University, Nanchong, China

First published on: 08 July 2010

To cite this Article Jiang, J. and Ai, L. H.(2010) 'Conducting Polymeric Nanocomposites: Preparation and Evaluation of Structural and Electromagnetic Properties', Molecular Crystals and Liquid Crystals, 524: 1, 179 — 187
To link to this Article: DOI: 10.1080/15421400903568153
URL: http://dx.doi.org/10.1080/15421400903568153

Mol. Cryst. Liq. Cryst., Vol. 524: pp. 179–187, 2010

ISSN: 1542-1406 print/1563-5287 online
DOI: 10.1080/15421400903568153

Taylor & Francis
Taylor & Francis Group

Conducting Polymeric Nanocomposites: Preparation and Evaluation of Structural and Electromagnetic Properties

J. JIANG AND L. H. AI

Chemical Synthesis and Pollution Control Key Laboratory of Sichuan Province, College of Chemistry and Chemical Engineering, China West Normal University, Nanchong, China

A facile rheological phase reaction method was developed to prepare the magnetic $Ni_{0.5}Zn_{0.5}Fe_2O_4$ nanoparticles (NZFO NPs). By an in situ *polymerization process, electromagnetic functionalized polyaniline/$Ni_{0.5}Zn_{0.5}Fe_2O_4$ nanocomposites (PANI/NZFO NCs) containing different contents of inorganic components were obtained. The effect of NZFO NPs content on the structure, morphology, and electromagnetic properties of PANI/NZFO NCs was investigated by modulating mass ratios of aniline monomer to NZFO NPs. The conductivity of PANI/NZFO NCs decreased with increasing content of NZFO NPs. The magnetic parameters such as saturation magnetization and coercivity of NZFO NPs decreased after PANI coating.*

Keywords Conducting polymer; conductivity; magnetic property; nanocomposite

Introduction

Inherently conducting polymers (ICPs) are attractive materials, because they cover a wide range of functions from insulators to metals and retain the mechanical properties of conventional polymers [1,2]. The considerable electrochemical and physicochemical properties result in conducting polymers having various practical applications, such as corrosion protection coatings, electrocatalysts, chemical sensors, rechargeable batteries, light-emitting diodes (LEDs), and electromagnetic interference (EMI) shielding [3–8]. Among the conducting polymers, polyaniline (PANI) has received a great deal of attention in recent years due to its easy synthesis, good environmental stability, and high electrical conductivity.

Organic–inorganic nanocomposites with an organized structure provide a new functional hybrid between organic and inorganic materials. Novel properties of these nanocomposites can be derived from the successful combination of the characteristics of individual constituents into a single material. Recently, many interesting research studies have focused on the PANI/transition metal (TM) oxide nanocomposites to obtain the materials with synergetic or complementary behavior between

Address correspondence to J. Jiang, Chemical Synthesis and Pollution Control Key Laboratory of Sichuan Province, College of Chemistry and Chemical Engineering, China West Normal University, Shida Road 1#, Nanchong 637002, China. E-mail: 0826zjjh@163.com

polyaniline and inorganic nanoparticles, including PANI/TiO_2 [9], PANI/SnO_2 [10], PANI/ZnO [11], PANI/Fe_3O_4 [12], PANI/CeO_2 [13], and PANI/Co_3O_4 [14].

Ferrite with a spinel structure that is formed by a nearly close-packed fcc array of anions with holes partly filled by the cations can be represented by the formula AB_2O_4, where A represents metallic ions located in A interstitial (tetrahedral) sites and B metallic ions located in B (octahedral) sites. Due to the large electronegativity of oxygen, the ionic type of bond prevails in almost all oxide spinels. Soft spinel ferrite (MFe_2O_4, M=Co, Ni, Zn, Mn, etc.) nanoparticles have been intensively investigated due to their remarkable magnetic and electrical properties and wide practical applications in ferrofluids, magnetic drug delivery, magnetic high-density information storage, and microwave absorbance [15–17]. Based on the above considerations we were motivated to design and fabricate a new class of functional materials combining conducting PANI with magnetic ferrite, which may find their potential applications in microwave absorbing and magnetoelectric devices.

In the present work, $Ni_{0.5}Zn_{0.5}Fe_2O_4$ nanoparticles (NZFO NPs) were chosen as a magnetic source due to their scientific and technological interest and excellent high microwave absorption performances, which was prepared by a facile rheological phase reaction method [18]. The nanocomposites were obtained by *in situ* polymerization of aniline in the presence of NZFO NPs. The effect of the content of NZFO NPs with respect to the electromagnetic properties of PANI/NZFO NCs is discussed on the basis of the structure characterization and morphology analysis.

Experimental

Materials

Aniline was distilled twice under reduced pressure and stored below 0°C. $Fe(NO_3)_3 \cdot 9H_2O$, $Ni(NO_3)_2 \cdot 6H_2O$, $Zn(NO_3)_2 \cdot 6H_2O$, $H_2C_2O_4 \cdot 2H_2O$, and ammonium peroxydisulfate (APS, $(NH_4)_2S_2O_8$) were all of analytical purity and used without further purification.

Preparation of NZFO NPS

NZFO NPs were prepared by a rheological phase reaction method. Stoichiometric amounts of $Fe(NO_3)_3 \cdot 9H_2O$, $Ni(NO_3)_2 \cdot 6H_2O$, $Zn(NO_3)_2 \cdot 6H_2O$, and $H_2C_2O_4 \cdot 2H_2O$ were mixed thoroughly and then were ground in an agate mortar for 30 min. The mixture was transferred into a 50-mL Teflon-lined stainless autoclave, and an appropriate amount of absolute ethanol was added to form a rheological state mixture. The autoclave was sealed and maintained in a furnace at 120°C for 48 h and then was cooled to room temperature naturally. The resulting solid product was collected by filtration, washed with deionized water and ethanol, and finally dried at 60°C for 12 h. The as-prepared precursors were calcined at 900°C for 2 h in air.

Preparation of PANI/NZFO NCS

PANI/NZFO NCs were prepared by *in situ* polymerization of aniline in the presence of NZFO NPs. In a typical procedure, a certain amount of NZFO NPs were added to 35 mL of 0.1 M HCl solution containing 1 mL of aniline monomer and stirred for 30 min. The 2.49 g of APS in 20 mL of 0.1 M HCl solution was then slowly added

dropwise to the suspension mixture with constant stirring. The polymerization was allowed to proceed for 12 h at room temperature. The nanocomposites were obtained by filtering and washing the suspension with deionized water and methanol and dried under vacuum at 60°C for 24 h. The nanocomposites with different content of NZFO NPs were synthesized by modulating mass ratios of aniline monomer to NZFO NPs at 9:1 (PANI/NZFO-1) and 4:1 (PANI/NZFO-2), respectively.

Characterization

The X-ray diffraction (XRD) patterns of the obtained products were collected on an X'pert Pro MPD diffractometer (Philips, The Netherlands) with Cu Kα radiation ($\lambda = 0.15418$ nm). Infrared spectra were recorded on an Avatar 360 (Nicolet, USA) spectrometer using KBr pellets. Scanning electron microscope (SEM) micrographs were obtained on a Hitachi S4800 scanning electron microscope (Hitachi, Japan). UV-Vis absorption spectra were recorded on a UV-2550 spectrophotometer (Shimadzu, Japan), using *N,N*-dimethylformamide (DMF) as the solvent. Magnetic measurements were carried out at room temperature using a Lakeshore 7404 vibrating sample magnetometer (Lakeshore, USA).

Results and Discussions

Formation Mechanism

Figure 1 illustrates the polymerization process for PANI/NZFO NCs. It is known that the surface charge of metal oxide is positive below the pH of the point of zero charge (PZC), whereas it is negative above that. Because the surface of magnetite has PZC of pH $\approx$ 6 [19], it is positively charged in acidic conditions. Therefore, adsorption of an amount of the anions may occur and compensate for the positive charges on NZFO NPs surface. Meanwhile, the specific adsorption of these anions on the NZFO NPs surface may also take place. In this approach, aniline monomers are converted to cationic anilinium ions in acidic conditions. Thus, the electrostatic interactions appear between anions adsorbed on the NZFO NPs surface and cationic anilinium ions. The aniline monomers electrostatically complexed to the NZFO NPs surface are then polymerized by ammonium persulfate as an oxidizing agent at room temperature.

Structural Characterization

Figure 2 shows XRD patterns of the NZFO NPs obtained by a rheological phase reaction method. The observed diffraction peaks are perfectly indexed to cubic spinel

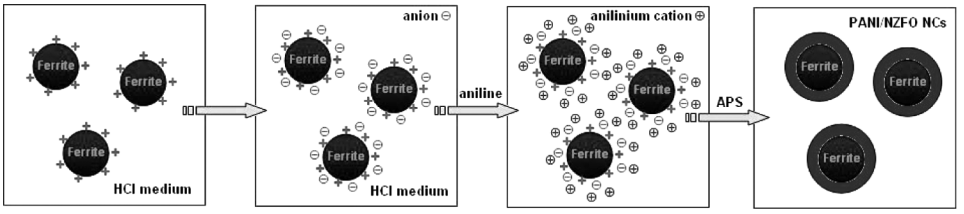

Figure 1. Formation process of PANI/NZFO NCs.

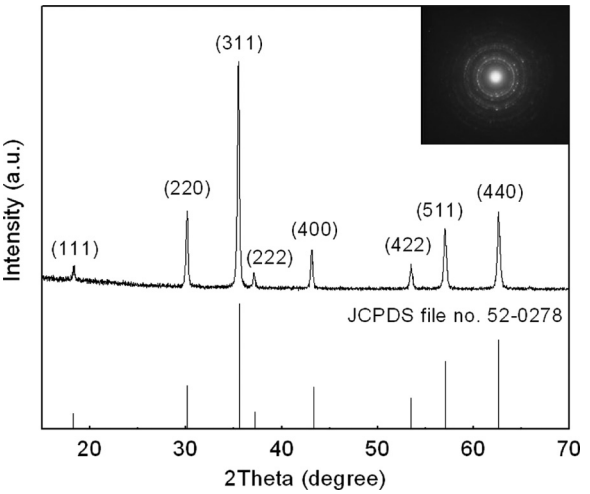

Figure 2. XRD patterns of the as-prepared NZFO NPs.

phase (JCPDS card No. 52-0278), and no impurities are detected in the XRD patterns. The sharp diffraction peaks indicate good crystallinity of the as-prepared product. In addition, the electron diffraction (ED) pattern shown in the upper right inset of Fig. 2 can be well indexed to (111), (220), (311), (222), (400), (422), (511), and (440) of cubic spinel structure, which is consistent with the results of XRD.

Figure 3 shows the XRD patterns of PANI/NZFO NCs. It is clearly seen that the characteristic peaks of PANI centered at around $2\theta = 20.1$, 25.1° and NZFO located at $2\theta = 30.2$, 35.6, 37.2, 43.3, 53.4, 57.1, and 62.6° appear in the XRD patterns of the nanocomposites. Also, the intensities of the characteristic peaks of PANI become weaker after introducing the NZFO NPs into the polymer matrix, revealing

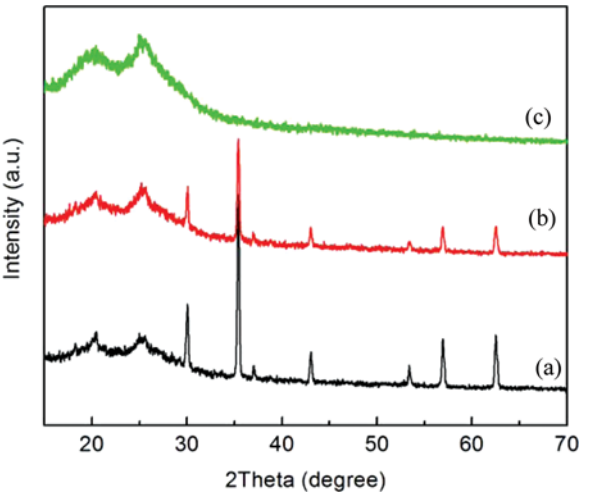

Figure 3. XRD patterns of PANI/NZFO-2 NCs (a), PANI/NZFO-1 NCs (b), and PANI (c).

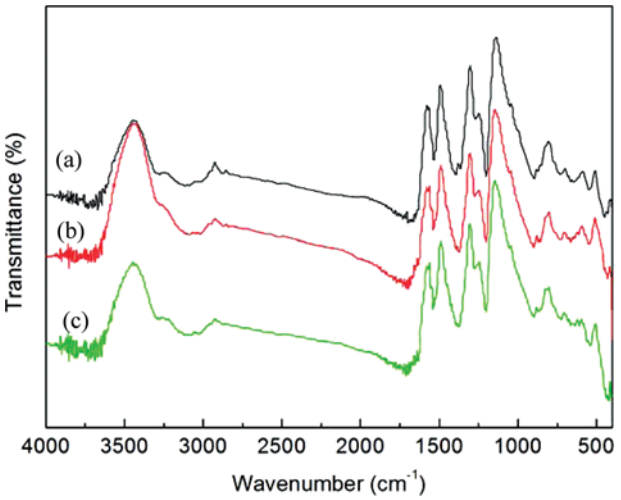

Figure 4. FTIR spectra of PANI (a), PANI/NZFO-1 NCs (b), and PANI/NZFO-2 NCs (c).

that the crystallinity of PANI in the nanocomposites is much lower than that of pristine PANI.

The Fourier transform infrared (FTIR) spectra measurement was carried out to study the molecular structure of the nanocomposites. Figure 4 shows the FTIR spectra of PANI/NZFO NCs. For the pristine PANI, the characteristic peaks observed at 1571 and 1493 cm^{-1} relate to the C=C stretching of the quinoid rings and benzenoid rings, respectively. The peaks at 1297 and 1242 cm^{-1} are attributed to the C−N stretching modes of the benzenoid ring. The broad peak appearing at 1134 cm^{-1} is assigned to the C−H in-plane bending modes. The peak at 802 cm^{-1} refers to the C−H out-of-plane bending modes. As shown in Figs. 4(b) and 4(c), the FTIR spectra of PANI/NZFO NCs are almost identical to that of the pristine PANI; moreover, the characteristic peak for NZFO NPs at around 618 cm^{-1} in the spectrum indicates the presence of NZFO in the PANI/NZFO NCs [20].

Figure 5 displays UV-Vis absorption spectra of PANI/NZFO NCs. For the pristine PANI, two characteristic absorption bands at around 346 and 605 nm can be observed in Fig. 5(a), which correspond to the π-π^* transition of the benzenoid ring and charge transfer from the benzenoid rings to the quinoid rings, respectively. It is interesting to note that the absorption peak at 346 nm corresponding to the pristine PANI has a red shift in the spectrum of PANI/NZFO NCs. These results suggest that there may be interaction between NZFO NPs and PANI molecular chains [21].

Morphology

The surface morphology of PANI/NZFO NCs was investigated by means of SEM. Figure 6(a) gives the SEM micrograph of the NZFO synthesized by a rheological phase reaction method, indicating that the sample consisted of a large quantity of quasi-spherical nanoparticles with size ranging from 80 to 100 nm. Due to the

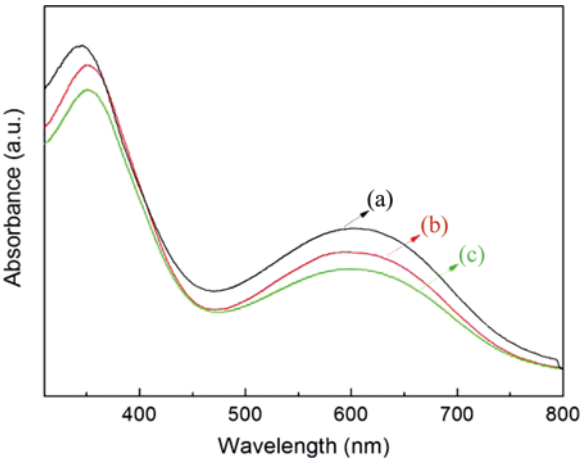

Figure 5. UV-Vis spectra of PANI (a), PANI/NZFO-1 NCs (b), and PANI/NZFO-2 NCs (c).

relatively higher annealing temperature and interaction between magnetic particles, some degree of agglomeration appears unavoidable. Figure 6(b) shows the SEM micrograph of PANI/NZFO NCs, suggesting that the fine PANI particles are deposited on the surface of NZFO NPs.

Electrical Properties

Figure 7 shows the conductivity of PANI/NZFO NCs at room temperature. It is observed that NZFO NPs have a significant influence on the conductivity of PANI/NZFO NCs. The conductivity of PANI/NZFO NCs greatly decreases with increasing content of NZFO NPs. These results can be considered as follows: (1) the insulting behavior of NZFO NPs in the nanocomposites; (2) from XRD study, the introduction of NZFO NPs would weaken the crystallinity of PANI; (3) a certain interaction between NZFO NPs and PANI chains further leads to destruction of the conjugated degree, continuity, and regularity of the polymer chains.

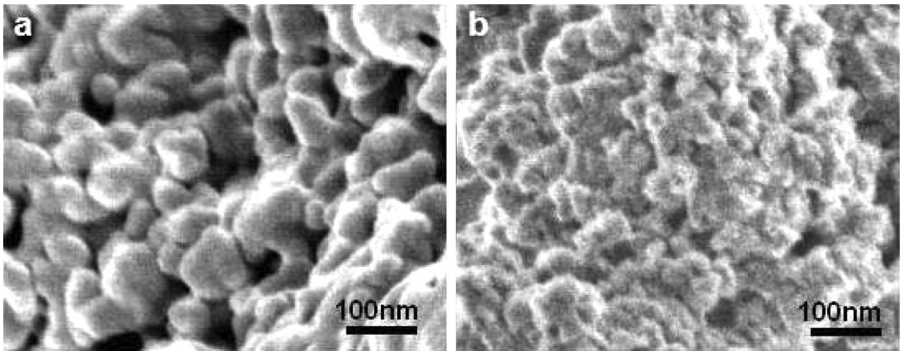

Figure 6. SEM micrographs of NZFO NPs (a) and PANI/NZFO-1 NCs (b).

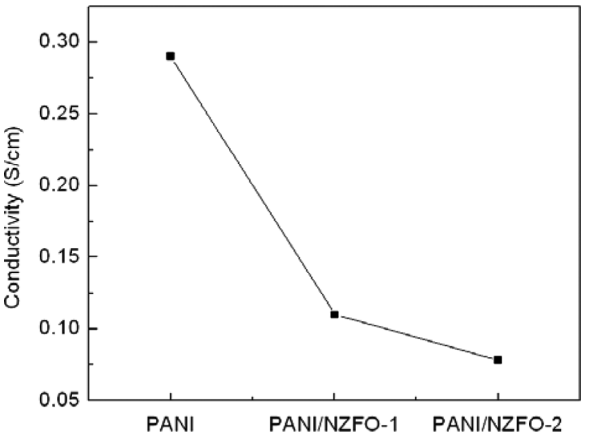

Figure 7. Conductivity of PANI, PANI/NZFO-1 NCs, and PANI/NZFO-2 NCs.

Magnetic Properties

The magnetization measurements for PANI/NZFO NCs were carried out using a vibrating sample magnetometer (VSM) at room temperature under an applied magnetic field. Figure 8 shows the magnetic hysteresis loops of PANI/NZFO NCs. It is clearly seen that the magnetic parameters such as saturation magnetization (M_S) and coercivity (H_C) determined by the hysteresis loops for the NZFO NPs decrease after polyaniline coating.

The decrease in M_S of PANI/NZFO NCs with decreasing NZFO NPs content shows that the NZFO NPs are responsible for the magnetic behavior of the nanocomposites; furthermore, it is interesting to note that the values of M_S of PANI/NZFO NCs are not proportional to the mass fraction of magnetic component

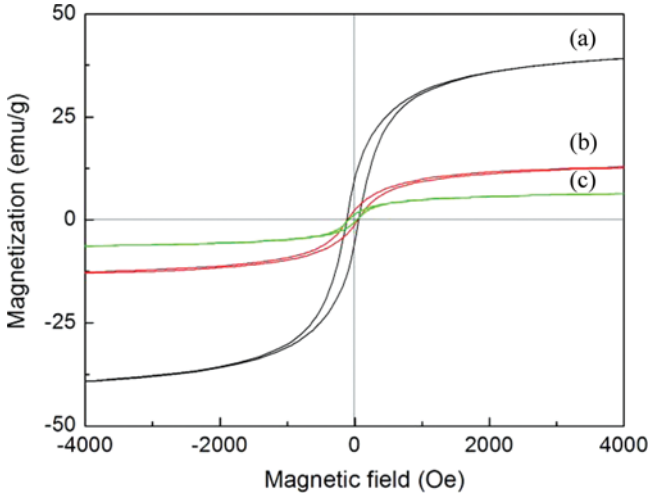

Figure 8. Hysteresis loops of NZFO NPs (a), PANI/NZFO-2 NCs (b), and PANI/NZFO-1 NCs (c).

in the PANI/NZFO NCs, due to a possible charge transfer between the NZFO surface and PANI, analogous to the corrosion protection of metals by depositing PANI [22].

Magnetic properties observed for magnetic materials are a combination of many anisotropy mechanisms, such as magnetocrystalline anisotropy, surface anisotropy, and interparticle interactions. An effective anisotropy constant, K_{eff}, is expressed as [23]:

$$K_{eff} = K + K_s + K_{sh} + K_{in} \quad (1)$$

where K_s is the constant of surface anisotropy, K_{sh} is the constant of shape anisotropy, and K_{in} is the (positive) constant of supplementary anisotropy that reflects nanocrystallite interactions. It is known that the surface anisotropy results from low coordination symmetry for spin–orbit couplings at the surface of nanoparticles and decreases upon coating; moreover, the interparticle interactions decrease when magnetic particles are coated with the nonmagnetic matrix due to the increase of particle–particle separation. In our case, the variation of K_{sh} for the NZFO NPs after coating with PANI may be ignored due to the spherical morphology of NZFO and PANI/NZFO NCs. Hence, according to Eq. (1), K_{eff} may decrease due to the reduction of surface anisotropy and interparticle interactions after PANI coating. On the basis of the above discussion, the decrease in coercivity of NZFO NPs after PANI coating is expected.

Conclusion

In summary, the electromagnetic functionalized PANI/NZFO NCs containing different content of NZFO NPs were successfully synthesized by *in situ* polymerization of aniline in the presence of NZFO NPs that were obtained by a facile rheological phase reaction method. The desired electrical and magnetic properties of PANI/NZFO NCs can be modulated simply by controlling the contents of NZFO NPs. The spectroanalysis confirmed that a certain interaction existed between NZFO NPs and PANI molecular chains. The conductivity of PANI/NZFO NCs decreased with increasing content of NZFO NPs. The saturation magnetization and coercivity of NZFO NPs decreased after PANI coating. The prepared nanocomposites may have potential applications in microwave absorbing and magnetoelectric devices.

Acknowledgments

This work was supported by Scientific Research Start-up Foundation of China West Normal University (07B008).

References

[1] MacDiarmid, A. G. (2001). *Angew. Chem. Inter. Ed.*, *40*, 2581.
[2] Bhadra, S., Khastgir, D., Singha, N. K., & Lee, J. H. (2009). *Progr. Polymer Sci.*, *34*, 783.
[3] Sathiyanarayanan, S., Azim, S. S., & Venkatachari, G. (2008). *Electrochim. Acta*, *53*, 2087.
[4] Bavio, M. A., Kessler, T., & Castro Luna, A. M. (2008). *J. Colloid Interface Sci.*, *325*, 414.

[5] Koul, S., Chandra, R., & Dhawan, S. K. (2001). *Sensor. Actuator. B*, *75*, 151.
[6] Rehan, H. H. (2003). *J. Power Sourc.*, *113*, 57.
[7] Yang, C.-H., & Yang, T.-C. (2008). *J. Phys. Chem. Solid*, *69*, 769.
[8] Mäkelä, T., Pienimaa, S., Taka, T., Jussila, S., & Isotalo, H. (1997). *Synth. Met.*, *85*, 1335.
[9] Sathiyanarayanan, S., Syed Azim, S., & Venkatachari, G. (2007). *Electrochim. Acta*, *52*, 2068.
[10] Geng, L., Zhao, Y., Huang, X., Wang, S., Zhang, S., & Wu, S. (2007). *Sensor. Actuator. B*, *120*, 568.
[11] Bhat, S. V., & Vivekchand, S. R. C. (2006). *Chem. Phys. Lett.*, *433*, 154.
[12] Lu, X., Mao, H., Chao, D., Zhang, W., & Wei, Y. (2006). *J. Solid State Chem.*, *179*, 2609.
[13] He, Y. (2005). *Mater. Chem. Phys.*, *92*, 134.
[14] Wang, S. X., Sun, L. X., Tan, Z. C., Xu, F., & Li, Y. S. (2007). *J. Therm. Anal.*, *89*, 609.
[15] Pileni, M. P. (2001). *Adv. Funct. Mater.*, *5*, 323.
[16] Cheng, F. Y., Su, C. H., Yang, Y. S., Yeh, C. S., Tsai, C. Y., Wu, C. L., Wu, M. T., & Shieh, D. B. (2005). *Biomaterials*, *26*, 729.
[17] Song, Q., & Zhang, Z. J. (2004). *J. Am. Chem. Soc.*, *126*, 6164.
[18] Jiang, J., & Yang, Y.-M. (2007). *Mater. Lett.*, *61*, 4276.
[19] Sun, Z. X., Su, F. W., Forsling, W., & Samskog, P. O. (1998). *J. Colloid Interface Sci.*, *197*, 151.
[20] Wuang, S. C., Neoh, K. G., Kang, E. T., Pack, D. W., & Leckband, D. E. (2007). *J. Mater. Chem.*, *17*, 3354.
[21] Yang, C., & Chen, C. (2005). *Synthetic Met.*, *153*, 133.
[22] Fahlman, M., Jasty, S., & Epstein, A. J. (1997). *Synthetic Met.*, *85*, 1323.
[23] Caizer, C., & Stefanescu, M. (2002). *J. Phys. Appl. Phys.*, *35*, 3035.